

## Upper mantle magma storage and transport under a Canarian shield-volcano, Teno, Tenerife (Spain)

Marc-Antoine Longpré,<sup>1</sup> Valentin R. Troll,<sup>1,3</sup> and Thor H. Hansteen<sup>2</sup>

Received 4 October 2007; revised 29 February 2008; accepted 27 March 2008; published 2 August 2008.

[1] We use clinopyroxene-liquid thermobarometry, aided by petrography and mineral major element chemistry, to reconstruct the magma plumbing system of the late Miocene, largely mafic Teno shield-volcano on the island of Tenerife. Outer rims of clinopyroxene and olivine phenocrysts show patterns best explained by decompression-induced crystallization upon rapid ascent of magmas from depth. The last equilibrium crystallization of clinopyroxene occurred in the uppermost mantle, from ~20 to 45 km depth. We propose that flexural stresses or, alternatively, thermomechanical contrasts create a magma trap that largely confines magma storage to an interval roughly coinciding with the Moho at ~15 km and the base of the long-term elastic lithosphere at ~40 km below sea level. Evidence for shallow magma storage is restricted to the occurrence of a thick vitric tuff of trachytic composition emplaced before the Teno shield-volcano suffered large-scale flank collapses. The scenario developed in this study may help shed light on some unresolved issues of magma supply to intraplate oceanic volcanoes characterized by relatively low magma fluxes, such as those of the Canary, Madeira and Cape Verde archipelagoes, as well as Hawaiian volcanoes in their postshield stage. The data presented also support the importance of progressive magmatic underplating in the Canary Islands.

**Citation:** Longpré, M.-A., V. R. Troll, and T. H. Hansteen (2008), Upper mantle magma storage and transport under a Canarian shield-volcano, Teno, Tenerife (Spain), *J. Geophys. Res.*, 113, B08203, doi:10.1029/2007JB005422.

### 1. Introduction

[2] The nature and dynamics of magma plumbing systems are key variables required to understand the behavior of overlying volcanic edifices. With the exception of a few intensely studied localities [e.g., *Pallister et al.*, 1992; *Tilling and Dvorak*, 1993], these variables are typically unconstrained at individual volcanoes worldwide. Where attempted, studies of magma storage and transport have revealed complex plumbing geometries in a range of geological settings [e.g., *Marsh*, 1996; *Andronico et al.*, 2005], indicating that assumptions of shallow, spherical-elliptical magma chambers may be generally oversimplified. A variety of techniques, ranging from remote geophysical monitoring of eruptions to studies of fluid inclusions trapped in minerals, can provide information on magma storage and transport and the rates at which these processes might occur [e.g., *Hansteen et al.*, 1998; *Amelung and Day*, 2002]. At highly active, basaltic shield-volcanoes, geophysical monitoring is an effective tool to investigate plumbing system geometries [e.g., *Peltier et al.*, 2007]. In the Canary

Islands, however, the low eruption frequency results in poor deformation and volcano-seismic data sets and, hence, volcanologists have to rely on alternative methods to study the magma plumbing system of Canarian volcanoes.

[3] The Teno massif, in northwest Tenerife, is the deeply eroded expression of a Miocene shield-volcano (Figure 1). At this locality, an initial subaerial edifice rapidly grew from ~6.3 to 6.1 Ma, building the Masca Formation [*Leonhardt and Soffel*, 2006; *Thirlwall et al.*, 2000; *Walter and Schmincke*, 2002; *Guillou et al.*, 2004]. *Walter and Schmincke* [2002] noted the presence of thick “phonolitic agglutinates”, near the top of this formation. This anomalously evolved unit among Teno volcanics is herein referred to as a vitric tuff of trachytic composition (Longpré et al., submitted manuscript, 2008). Subsequently, the volcano was affected by two large-scale flank collapses, marked by steep angular unconformities consisting mainly of polymict breccia [*Walter and Schmincke*, 2002]. Edifice regrowth occurred after each landslide, resulting in two ~700-m-thick sequences of subhorizontal lavas. The Carrizales Formation (after the first, Masca Collapse) and the El Palmar Formation (after the second, Carrizales Collapse) appear to have been erupted in a short, ~250 ka, time interval [*Leonhardt and Soffel*, 2006]. The Los Gigantes Formation, the outermost and youngest Miocene volcanics at Teno, is conformably capping the Masca Formation and may have been emplaced after a possible hiatus in activity of up to ~0.5 Ma [*Guillou et al.*, 2004; *Leonhardt and Soffel*, 2006]. Pleistocene cinder cones and lava flows, associated with the Northwest

<sup>1</sup>Department of Geology, Trinity College Dublin, Dublin, Ireland.

<sup>2</sup>IFM-GEOMAR, Leibniz-Institut für Meereswissenschaften, Kiel, Germany.

<sup>3</sup>Now at Department of Earth Sciences, Uppsala Universitet, Uppsala, Sweden.

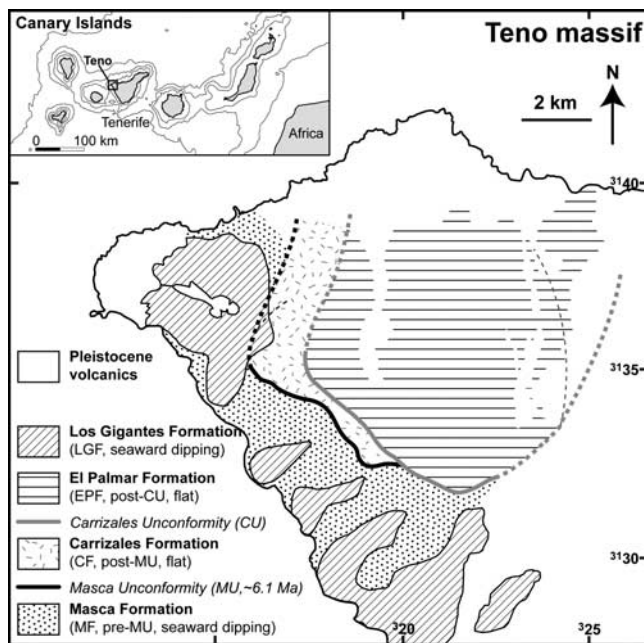


**Figure 1.** Geological map of the Teno massif, adapted from *Walter and Schmincke* [2002], *Carracedo et al.* [2007], and Longpré et al. (submitted manuscript, 2008).

Rift of the Las Cañadas and Pico Viejo-Teide central edifices, are sparsely distributed in the northern and western parts of the massif [*Carracedo et al.*, 2007]. Teno lavas include abundant alkali basalts and picrobasalts (often ankaramites), common basanites and less frequent, more evolved hawaiites, mugearites and benmoreites [*Thirlwall et al.*, 2000]. *Neumann et al.* [1999] argued that fractional crystallization of periodically refilled crustal magma chambers is the major process influencing the geochemical character of Tenerife lavas. Conversely, *Thirlwall et al.* [2000] proposed that the chemistry of the shield massif volcanics in Tenerife is dominantly controlled by variation in depth and extent of melting followed by mineral fractionation and accumulation.

[4] In this paper, we use chemical thermobarometry, based on clinopyroxene-melt equilibria [*Putirka et al.*, 1996] and supported by petrography and mineral chemistry, to reconstruct the magma plumbing system of the Teno volcano at the time of emplacement of the El Palmar Formation, i.e., the lavas erupted after the second collapse. Information on local edifice, oceanic crust and upper mantle structure is integrated with P-T estimates to investigate controls on magma storage and transport at this Miocene volcano.

## 2. Methods

### 2.1. Sampling

[5] Unaltered El Palmar lava flows were systematically sampled mainly from a particularly well-exposed stratigraphic profile that directly overlies the second angular unconformity (main profile from UTM coordinates [318090, 3134110] to [317460, 3135620] (datum WGS84)). Overall, our sample set spans a total stratigraphic height of ~400 m.

On the basis of outcrop modal mineralogy, this sequence is divided into two broad groups: (1) a lower part, with highly clinopyroxene-olivine-phyric (>20 vol. %) lavas (ankaramites), and (2) an upper part, mainly consisting of nearly aphyric (<5 vol. %) to moderately clinopyroxene- and/or olivine- and/or plagioclase-phyric (5–20 vol. %) basaltic lavas.

### 2.2. Analytical Procedure

[6] Whole-rock major element compositions were obtained for all samples, using the X-Ray Fluorescence facility at IFM-GEOMAR (see procedure details by *Abratis et al.* [2002]). In addition, groundmass material was extracted for ankaramitic samples. These microcrystalline groundmass separates were powdered to the nm-scale and subsequently fused on an Ir-filament and quenched to glass under air at the Institute of Mineralogy, University of Frankfurt. The glass shards obtained were analyzed in 10 points for major element composition with a CAMECA SX-50 electron microprobe (EMP) at IFM-GEOMAR, following the procedure outlined by *Klügel et al.* [2005]. Alkali loss was minimized by using a defocused beam ( $3 \times 4 \mu\text{m}$ ) of 10 nA. Phenocrysts were analyzed by EMP in core-to-rim profiles of 10 to 50 points with two to five additional rim analyses per crystal, using a focused beam with a current of 20 nA.

### 2.3. Data Filtering

[7] The results presented in this paper include data from 80 clinopyroxene and 55 olivine phenocrysts from a total of 12 rock samples. The compositions of fused groundmass glass shards were verified to be homogeneous and were averaged for each sample (Longpré et al., submitted manuscript, 2008). We confirmed that alkali loss was negligible by verifying that the fused groundmass compositions fall on the liquid line of descent for Teno magmas using our whole-rock analyses and data from *Thirlwall et al.* [2000] and *Neumann et al.* [1999]. Clinopyroxene analyses were quality controlled by selecting only those yielding sums approaching 100%, 0 wt %  $\text{K}_2\text{O}$  and four cations per six oxygens.

### 2.4. Thermobarometry and Uncertainties

[8] *Putirka et al.* [1996] developed expressions based on the jadeite-diopside/hedenbergite-liquid and jadeite-liquid exchange equilibria that can respectively be used as thermometers and thermobarometers of clinopyroxene-melt equilibration. The uncertainties associated with these formulations are  $\pm 27^\circ\text{C}$  and  $\pm 140 \text{ MPa}$ .

[9] Validity of equilibrium conditions between clinopyroxenes and host melt (fused groundmass and whole-rock compositions for ankaramitic and basaltic samples, respectively) was assessed by comparing the observed clinopyroxene  $\text{Mg}\# = \text{molar Mg}/(\text{Mg} + \text{Fe}_{\text{tot}}) \times 100$  to the clinopyroxene  $\text{Mg}\#$  predicted by the formulations of *Duke* [1976] and *Putirka* [1999] (Figure 2a). If the ratio  $\text{Mg}\#_{\text{observed}}/\text{Mg}\#_{\text{predicted}} = 1 \pm 0.05$  the compositions of the clinopyroxene and the melt were considered to be in chemical equilibrium [cf. *Klügel et al.*, 2000, 2005; *Maclennan et al.*, 2001; *Schwarz et al.*, 2004]. If this ratio did not satisfy the above criterion, the P-T estimate was discarded. A possible source of uncertainty here resides in the potential effect of the presence of ferric iron in

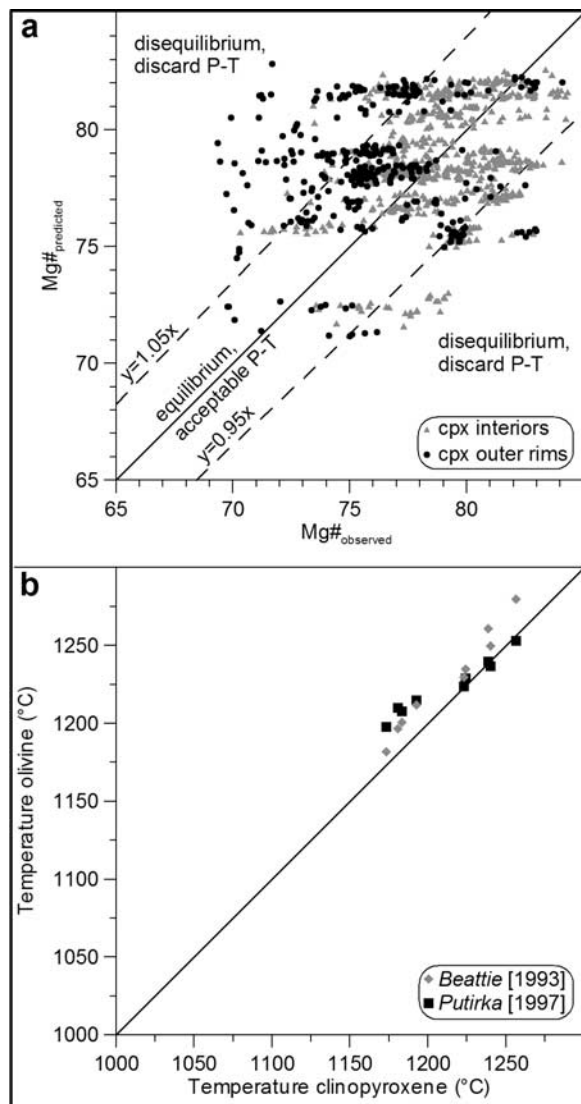


**Figure 2.** (a) Equilibrium test, predicted versus measured clinopyroxene Mg#. In this test, the predicted Mg# is calculated using the equation (3.3) of Putirka [1999]. A second test, using the formulation of Duke [1976], was also applied. Overall, 76% of the 1078 clinopyroxene analyses indicated equilibrium. See text for details. (b) Intracample average crystallization temperatures of olivine versus those of clinopyroxene.

both clinopyroxene and host melt. Although of doubtful accuracy [see McGuire *et al.*, 1989], the methods of Lindsley [1983] and Droop [1987] indicate that significant amounts of  $\text{Fe}^{3+}$  are required for clinopyroxene charge balance. On the basis of previous redox state investigations of Canary Island magmas [e.g., Gurenko *et al.*, 1996; Klügel *et al.*, 2000], we assumed  $f_{\text{O}_2} = \text{QFM} + 1$  and calculated (using the model of Kress and Carmichael [1988]) that Teno magmas may have had  $\text{Fe}_2\text{O}_3/\text{FeO}_{\text{tot}}$  wt % ratios between 0.10 and 0.12. However, since the effect of redox conditions were not explored by Duke [1976] and Putirka [1999], all iron was treated as divalent in the clinopyroxene equilibrium tests [cf. Schwarz *et al.*, 2004].

[10] As most samples contained olivine, we further tested the consistency of the data by comparing calculated crystallization temperatures of olivine [Beattie, 1993; Putirka, 1997] to those of clinopyroxene [Putirka *et al.*, 1996]. For this purpose, we selected olivine analyses yielding  $K_D^{\text{ol-liq}}[\text{Mg-Fe}^{2+}] = 0.30 \pm 0.03$  [Roeder and Emslie, 1970]. This test indicates compatible intrasample crystallization temperatures for both mineral phases (Figure 2b). Thermometers of Beattie [1993] and Putirka [1997] estimate crystallization temperature of olivine with uncertainties of  $\pm 10$  and  $\pm 31^\circ\text{C}$ , respectively.

[11] Note that the thermobarometers are expected to be applicable to a wide range of  $f_{\text{O}_2}$ , encompassing that inferred for Teno magmas [cf. Putirka *et al.*, 2003]. Moreover, Maclennan *et al.* [2001] found that the presence of  $\text{Fe}^{3+}$  in clinopyroxene was unlikely to yield overestimated pressure results [cf. Neumann *et al.*, 1999]. Also, Klügel *et al.* [2005] and Mordick and Glazner [2006] showed that, if the analytical error is low, the thermobarometric calculations using the formulations of Putirka *et al.* [1996] can be considered precise and accurate.

## 2.5. Pressure to Depth Conversion

[12] Pressure is converted to depth by assuming a volcanic edifice height of 5.5 km with an average density of  $2600 \text{ kg/m}^3$  [Collier and Watts, 2001], a thick prevolcanic sediment cover and igneous oceanic crust with a total thickness of 11 km with an average density of  $2700 \text{ kg/m}^3$  [cf. Watts *et al.*, 1997; Ranero *et al.*, 1995] and an average upper mantle density of  $3240 \text{ kg/m}^3$  [Ranero *et al.*, 1995]. Atmospheric pressure thus corresponds to the Miocene volcano summit  $\sim 1.5$  km above present sea level, with the Moho situated at 15 km below present sea level [Banda *et al.*, 1981; Watts *et al.*, 1997].

## 3. Results

### 3.1. Petrographic Observations

[13] Clinopyroxene phenocrysts are generally euhedral to subhedral and display concentric optical zoning. A ubiquitous feature in virtually all clinopyroxene phenocrysts from both sample groups is the occurrence of conspicuous outer rims, characterized by a slightly darker color. Often, these rims host microcrysts of acicular apatite and prismatic magnetite. At high-magnification, these rims are commonly observed interlocking with laths of matrix plagioclase and sometimes forming dendritic protrusions (Figure 3a). Olivine phenocrysts are mostly euhedral and optically homogeneous, except for a slight change in birefringence commonly observed at their outer rims. Notably, glomerocrysts are extremely rare in thin section. The microcrystalline matrix of lava samples contains varying proportions of plagioclase laths, Fe-Ti oxides, clinopyroxene microphenocrysts and cryptocrystalline material. Accessory apatite is present and some rare olivine microphenocrysts are seen in some samples.

### 3.2. Mineral Chemistry

[14] Chemical profiles of clinopyroxene phenocryst interiors indicate generally constant, but locally slightly fluctuating major element compositions. Overall, variations in clinopyroxene components are limited to the range  $\text{Wo}_{43-50}$ ,

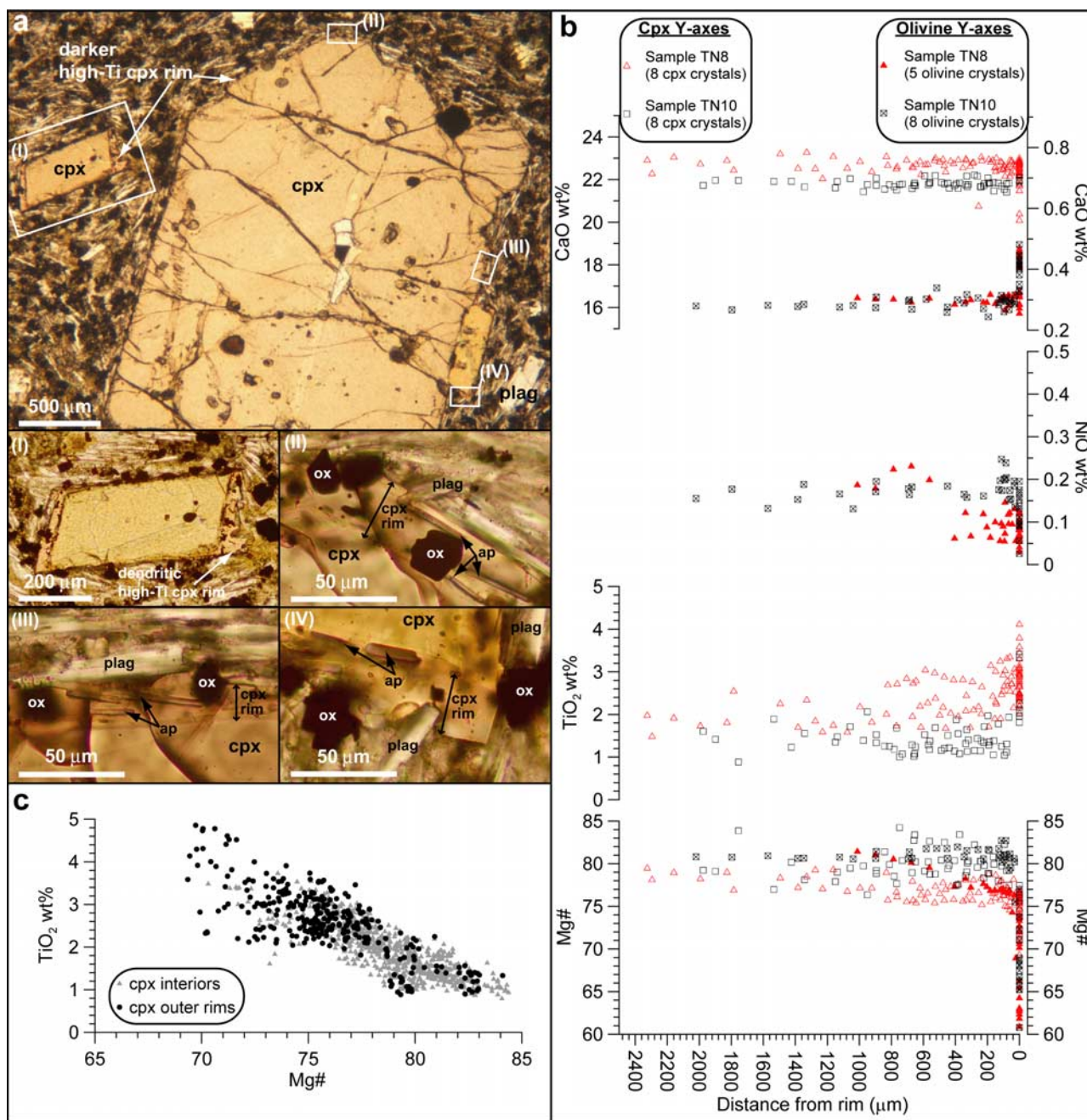


**Figure 3.** (a) Photomicrographs showing the darker coloration at the outer rims of clinopyroxenes, the acicular apatite and Fe-Ti oxide inclusions and an example of a dendritic protrusion. (b) Core-to-rim major element chemistry of clinopyroxene and olivine phenocrysts from representative samples TN8 and TN10. Note the relatively homogeneous composition of intrasample clinopyroxenes and olivines and the steep normal zoning at their rims. (c) TiO<sub>2</sub> wt % versus Mg# for the El Palmar Formation clinopyroxenes.

En<sub>35–43</sub>, Fs<sub>8–15</sub>, approaching the composition of diopside. In addition, the composition of olivine interiors is remarkably homogeneous at both the crystal and sample scales. However, both clinopyroxene and olivine commonly show steep normal Fe-Mg zonations, typically 20–40 μm wide, at their outer rims (Figure 3b). TiO<sub>2</sub> is inversely correlated with Mg# in clinopyroxene and often increases considerably at the rims (Figure 3c). Na-salite (green-core clinopyroxenes rich in Na<sup>2+</sup> and Fe<sup>3+</sup>), characterized by relatively low Mg#

cores and steep reverse zoning at their rims (Al-salite) as reported by *Neumann et al.* [1999], were not observed in our sample set.

### 3.3. Thermobarometry

[15] Following from several previous workers [e.g., *Schwarz et al.*, 2004; *Klügel et al.*, 2005; *Mordick and Glazner*, 2006], our approach isolates each clinopyroxene crystal and corresponding host melt as a system from which

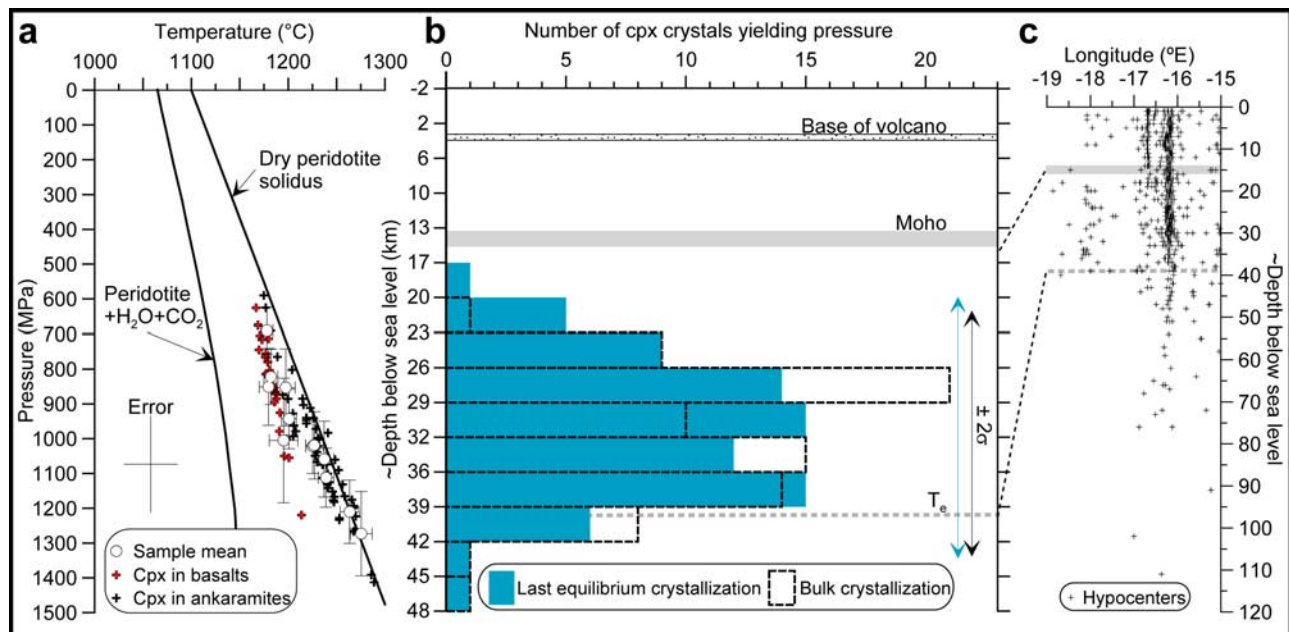


**Figure 4.** (a) P-T of clinopyroxene last equilibrium crystallization calculated by chemical thermobarometry. Data points from phenocryst-melt pairs indicated as crosses have uncertainties (labeled *error*) of Putirka *et al.*'s [1996] models. Sample means (circles) are also shown with  $\pm 1\sigma$  bars. The dry peridotite and peridotite + H<sub>2</sub>O + CO<sub>2</sub> solidi are plotted for comparison [Olafsson and Eggler, 1983; McKenzie and Bickle, 1988]. (b) Histograms compiling pressure estimates for the last equilibrium crystallization and the bulk crystallization. Data are plotted with respect to the pressure Y axis of Figure 4a. The equivalent rounded depth estimates are indicated relative to present sea level on the Y axis in Figure 4b. For example, read that one crystal yielded last equilibrium crystallization pressure between 500 and 600 MPa (depth between 17 and 20 km), whereas pressures between 800 and 900 MPa (depth between 26 and 29 km) were obtained for the bulk crystallization of 21 phenocrysts. The approximate depths of the base of the volcanic edifice, the Moho and the base of the long-term elastic lithosphere are indicated. (c) Hypocenter depths for the period 1975–2007 in the Canary Island region ( $-19^{\circ}$  to  $-15^{\circ}$ E,  $25^{\circ}$  to  $32^{\circ}$ N), giving an indication of the extent of brittle behavior. The data from Instituto Geográfico Nacional show 91% of events for which a depth was calculated clustering above 40 km depth.

P-T conditions may be estimated. Thermobarometric calculations, using the outermost phenocryst composition in equilibrium with the corresponding melt, indicate that the last equilibrium crystallization of the 80 clinopyroxene crystals occurred at pressures and temperatures ranging from 590–1410 MPa (mean = 970 MPa; standard deviation ( $\sigma$ ) = 187 MPa) and 1170–1290°C (Figures 4a and 4b). Although an almost complete overlap in calculated pressures exists between the basaltic and ankaramitic samples, the latter appear to have crystallized at slightly higher temperatures. Crystallization temperatures calculated for olivine are similar to those of clinopyroxene with ranges of 1180–1280°C and 1200–1260°C, using the thermometers of Beattie [1993] and Putirka [1997], respectively.

[16] As the analysis of Putirka *et al.* [2003] suggests, the average calculated pressure for all analyses that yield equilibrium within a crystal may serve as a representative value of the bulk crystal growth history. This is hereafter referred to as “bulk crystallization”. Calculations of bulk crystallization conditions of the phenocrysts show similar results to that of the last equilibrium crystallization with P-T ranges of 630–1440 MPa (mean = 990 MPa;  $\sigma$  = 177 MPa; Figure 4b) and 1170–1290°C.

[17] Alternatively, a more macroscopic method may be adopted, which considers the magma as a whole; in this case, all equilibrium P-T values for all clinopyroxenes in a rock/lava sample may be taken as equally valid. Sample means of equilibrium pressures and temperature and associated standard deviations are also plotted in Figure 4a. In comparison with the P-T of last equilibrium crystallization, this approach is found to yield essentially equivalent results.

## 4. Discussion

### 4.1. Magma Ascent

[18] Petrographic observations show that clinopyroxenes in late Teno lavas display overgrowth rims that appear to have crystallized rapidly. Indeed, the occurrence of widespread acicular apatite inclusions within and some dendritic protrusions on phenocryst and microphenocryst rims points toward accelerated growth rates and potentially even quench conditions [Wyllie *et al.*, 1962; Lofgren, 1974; Wass, 1979; Humphreys *et al.*, 2006]. In addition, the clustering of Fe-Ti oxide microcrystals within the outer rims of the clinopyroxenes suggests a change to a multiply saturated system; perhaps due to a variation in pressure, temperature

and/or oxygen fugacity [cf. *Perugini et al.*, 2003]. Moreover, the passive enrichment of Ti and Fe<sup>3+</sup> in the melt during prolonged olivine and clinopyroxene crystallization may have favored last-stage Ti-magnetite precipitation and is probably responsible for the high-Ti content and the distinctive coloration of the clinopyroxene outer rims [e.g., *Wass*, 1979].

[19] The steep normal Fe-Mg zoning associated with the darker tinged rims is, compared with the chemistry of clinopyroxene interiors, out of equilibrium with the melt (Figures 2a and 3b). The even steeper zonations at the rims of olivines have similar widths (on the order of 20–40  $\mu\text{m}$ ) to those observed on clinopyroxenes. This suggests that the zonations are related to growth rather than diffusion, as volume diffusion rates under these conditions would be about two orders of magnitude higher in olivine than in clinopyroxene [*Freer*, 1981]. The comparable zonation widths for Fe-Mg, Ca, Ni and Ti (Figure 3b), despite distinct diffusion coefficients for these elements [e.g., *Freer*, 1981], further support this interpretation. *Klügel et al.* [2000], based on such diffusion kinetics arguments, quantified the time-scales involved in the formation of essentially identical zonations in olivines from Cumbre Vieja volcano on the island of La Palma. These authors suggested that the zonations most probably formed during accelerated crystal growth over the course of a few days at most; such time-scales thus appear likely for the growth of Teno's El Palmar phenocryst rims.

[20] Exsolution of volatiles upon magma decompression is a well-documented cause of rapid crystallization of plagioclase in hydrous, dacitic magma [e.g., *Blundy and Cashman*, 2005]. However, the phase relations of *Rutherford et al.* [1985] imply that precipitation of other anhydrous phases, such as pyroxenes and Fe-Ti oxides, should also be favored and/or accelerated by magma ascent and degassing. Moreover, observations by *Sparks and Pinkerton* [1978] and *Lipman et al.* [1985] suggest that this mechanism also applies to basaltic magmas, and may result in the precipitation of clinopyroxene and olivine, in addition to plagioclase.

[21] Although H<sub>2</sub>O (and SO<sub>2</sub>) may degas mostly at shallow levels just before or upon eruption [*Gurenko and Schmincke*, 2000], Canarian mafic alkalic melts with ~1% dissolved CO<sub>2</sub> probably begin to exsolve a CO<sub>2</sub>-H<sub>2</sub>O fluid phase (containing some ~90% CO<sub>2</sub>, ~10% H<sub>2</sub>O [cf. *Sachs and Hansteen*, 2000]) at pressures in excess of 1000 MPa [cf. *Dixon*, 1997; *Hansteen et al.*, 1998, and references therein]. Degassing thus starts at upper mantle levels, but is enhanced and becomes progressively enriched in H<sub>2</sub>O during magma ascent [cf. *Dixon*, 1997], resulting in substantial magma undercooling. We therefore propose that out-of-equilibrium, decompressional crystallization, associated with degassing and large degrees of undercooling, resulted in the rapid growth of clinopyroxene and olivine rims [cf. *Klügel et al.*, 2000]. This mechanism may also have played a role in saturation of Fe-Ti oxides and plagioclase.

#### 4.2. Thermobarometric Approach and Magma Storage

[22] The thermobarometers of *Putirka et al.* [1996] require the input of suitable melt and clinopyroxene compositions. *Putirka* [1997] notes: “the limiting condition for extracting P-T information is that magma and coexisting crystals have approximated a closed equilibrium system

which has recorded a period of magma storage and pyroxene growth”. To date, the calculations have been applied to different melt compositions such as basalt, basanite and tephrite [e.g., *Putirka*, 1997; *Klügel et al.*, 2000]. Major element compositions of whole-rock (sometimes corrected for the presence of phenocryst phases other than clinopyroxene), natural glass or fused groundmass samples may be used as input melt [e.g., *Putirka*, 1997; *Schwarz et al.*, 2004; *Mordick and Glazner*, 2006]. Pressures have been quoted for phenocryst rims, cores, grain averages and sample averages.

[23] In this study, we used whole-rock and fused groundmass compositions to approximate the melt compositions for basaltic and ankaramitic samples, respectively. By analyzing the groundmass separates for the ankaramites, we ensured that the melt composition is not controlled by the presence of abundant phenocrysts that appear to have accumulated in suspension in the magma chamber [cf. *Thirlwall et al.*, 2000]. Our equilibrium tests and mineral chemistry data show that the fused groundmass composition is an accurate representation of the liquid that was in equilibrium with the clinopyroxenes and validates our approximation (Figures 2 and 3b).

[24] The last episode of equilibrium crystal growth may be recorded in the outer rims of phenocrysts, providing information on the P-T conditions prevailing just prior to final magma ascent and eruption. As commonly encountered in our data set, however, it is possible that the phenocryst rims show signs of disequilibrium with the melt, texturally and/or chemically, while the remainder of the crystal profile may indicate equilibrium (Figures 2a and 3b). Thermobarometric calculations using the composition of such rims may lead to potentially meaningless P-T estimates as the required conditions for the use of the thermobarometer are not satisfied. To overcome this problem, we have selected the outermost composition(s) (for each clinopyroxene phenocryst) yielding equilibrium Mg<sup>#</sup><sub>observed</sub>/Mg<sup>#</sup><sub>predicted</sub> ratio(s) to obtain the P-T value(s) of the “last equilibrium crystallization”. If multiple analyses satisfy the criterion, the mean of the corresponding calculated pressures and temperatures is used. If rim analyses do not satisfy the criterion, the analysis that indicates equilibrium closest to the rim is selected. This usually represents the analysis directly preceding the outer rim analyses, some tens of microns away.

[25] Our equilibrium tests show that, in most phenocrysts, several analyses along a core-to-rim profile indicate equilibrium with the melt [cf. *Mordick and Glazner*, 2006]. This is illustrated in the mineral chemistry data (Figure 3b); indeed, the concentric optical zoning observed in most clinopyroxene phenocryst interiors translates into very limited compositional fluctuations. As noted by *Thirlwall et al.* [2000], we emphasize the remarkable compositional similarity of clinopyroxene interiors. Under these inferred conditions, the homogeneity of olivine interiors may be expected from its simpler crystal structure (relative to clinopyroxene). We note, however, that this homogeneity may also partly reflect olivine's aptitude for rapid internal diffusion at high magmatic temperatures [e.g., *Freer*, 1981].

[26] We thus propose that the clinopyroxenes coexisted for the bulk of their growth history with a liquid of chemical composition closely approaching the final (erupted) melt

composition (in our case that of the fused groundmass or the whole-rock). Teno's mafic magmas may therefore have been crystallizing in fairly stagnant reservoirs, but characterized by frequent influx of fresh mafic melt normalizing the system's composition [cf. O'Hara, 1977; Neumann *et al.*, 1999]. The inferred rapid ascent of magmas may have disabled volumetrically significant phenocryst crystallization *en route* to eruption (only the outer rims) and hence preserved the main features of pre-ascent melt chemistry. In this context, P-T histories extracted from clinopyroxene phenocrysts may be valid not only for the outermost composition of a crystal. The similarity of the "bulk crystallization" and "last equilibrium crystallization" histograms (Figure 4b) would thus indicate that very few crystals have crystallized at successively lower pressures.

[27] Equilibrium crystallization pressures determined for phenocrysts from lavas of the El Palmar Formation indicate that long-term magma storage beneath Teno occurred virtually exclusively at depths of 20 to 45 km below sea level. Such uppermost mantle magma storage is in agreement with the occurrence of mantle xenoliths on several of the Canary Islands. Indeed, these rocks, which commonly show pervasive overprinting from basaltic melts, have been interpreted as wall rocks of upper mantle magma reservoirs at depths down to about 35 km [Neumann, 1991; Hansteen *et al.*, 1998], providing strong indirect support for the range of storage depths reported here for the Teno edifice. Teno's upper mantle magma plumbing system may have consisted of a plexus of discrete sill-like and dike-like magma-filled fractures, some of which were most probably interconnected. Similar models sharing some similarities with a magma mush column [Marsh, 1996] have been proposed for the westernmost Canary Islands, La Palma and El Hierro, and for the Madeira Archipelago, where upper mantle magma storage depths were also evidenced [Schwarz *et al.*, 2004; Klügel *et al.*, 2005; Stroncik *et al.*, submitted manuscript, 2008]. Mantle-level clinopyroxene crystallization/fractionation is also thought to be an important process at Hawaii (e.g., Mauna Kea volcano [Frey *et al.*, 1990]) and Iceland (e.g., Krafla and Theistareykir volcanic systems [MacLennan *et al.*, 2001]). Although we envisage the plumbing system of the Teno volcano to be similar to that of Cumbre Vieja volcano on the island of La Palma [cf. Klügel *et al.*, 2005], we note the following distinctive characteristics: (1) the main level of magma storage/crystallization is located at slightly greater depths at Teno; (2) the relatively homogeneous character of the El Palmar Formation phenocrysts may indicate comparatively large and homogeneous individual reservoirs; (3) the lack of low Mg#, greenish clinopyroxene (i.e., green-core or Na-salite) may assign a minimal role to mixing between more evolved magmas and Teno's mafic El Palmar magmas, contrasting with observations at several other Canarian volcanoes [cf. Neumann *et al.*, 1999; Klügel *et al.*, 2000; Troll and Schmincke, 2002].

[28] Coupled with the evidence for rapid magma ascent preserved in the phenocryst outer rims, our thermobarometric data imply that Teno magmas must have ascended from mantle depths within days. Short term, shallow (within volcanic edifice and upper crust) stagnation of magmas before eruptions may have occurred on timescales on the order of hours to days at most. However, our data do not

exclude magmatic intrusions becoming arrested at crustal levels without leading to eruptions, as previous studies have suggested it might be the case for most dikes [e.g., Gudmundsson *et al.*, 1999]. During the time of emplacement of the El Palmar Formation, however, it appears that the intrusions that fed eruptions were able to rapidly propagate from upper mantle depths to the surface.

[29] Our data partly contrast with initial results reported by Neumann *et al.* [1999] for Teno and other localities on Tenerife. These authors concluded, on the basis of the statistical approach of Soesoo [1997] and calculations using the MELTS models [Ghiorso and Sack, 1995], that crystallization most likely took place at pressures between 200 and 500 MPa, corresponding to depths within the volcanic edifice to the base of the oceanic crust. However, by comparing the Soesoo [1997] results with experimental data of Thompson [1974] for alkalic melts, Greenwood [2001] suggested that the Soesoo [1997] method might underestimate pressure by ~400 MPa. Moreover, Putirka *et al.* [2003] showed that the use of the MELTS models to calculate crystallization conditions cannot be recommended. On the other hand, the Putirka *et al.* [1996] approach appears to provide the most precise and accurate clinopyroxene thermobarometers available for mafic compositions [MacLennan *et al.*, 2001; Putirka *et al.*, 2003; Klügel *et al.*, 2005; Mordick and Glazner, 2006]. When using the Putirka *et al.* [1996] formulations, Neumann *et al.* [1999] obtained pressure ranges for Teno lavas nearly identical to the results presented in this study. Neumann *et al.* [1999] moreover supported their low pressure estimates using fluid inclusion microthermometry on gabbroic and nepheline syenite xenoliths, but were not able to perform this technique on magmatic phenocrysts. As the xenoliths may have been entrained at a late stage by ascending magmas and considering that fluid inclusions have the ability to rapidly reequilibrate to lower pressures [see, e.g., Hansteen *et al.*, 1998], the microthermometry data obtained by Neumann *et al.* [1999] do not exclude main storage at deeper levels for the host magmas. Although shallow storage has probably been an important process for the younger Las Cañadas and Pico Viejo-Teide edifices [e.g., Martí *et al.*, 1994; Ablay *et al.*, 1998; Carracedo *et al.*, 2007], we do not consider the evidence presented by Neumann *et al.* [1999] conclusive for the Teno volcano.

#### 4.3. Plumbing System Evolution at Ocean Island Volcanoes

[30] The archetypal "hot spot" volcanoes, the Hawaiian volcanoes, grow through four stages (the preshield, shield, postshield and rejuvenated (or posterosional) stages), for which magma supply rates, storage system configuration and erupted lava types (and entrained xenoliths) differ considerably [e.g., Clague, 1987]. In spite of low magma supply rates during the first, preshield stage, a "deep magma reservoir", perhaps near the crust-mantle interface, begins to form. This allows appreciable differentiation of alkalic magmas [Clague and Dixon, 2000]. During the main shield stage, sustained supply of tholeiitic magma results in rapid volcano growth and formation of shallow magma chambers as the temperature of the crust is sufficiently high to prevent magma solidification [Clague and Dixon, 2000]. Magma supply rates greatly diminish early in the postshield

stage, causing magma reservoirs and conduits in the edifice and upper crust to freeze. Only the “deep magma reservoir” persists until late in this evolutionary phase. The postshield stage of growth is particularly well-documented at Mauna Kea volcano, where fractionation of clinopyroxene-rich assemblages in the uppermost mantle ( $\sim 800$  MPa) is inferred to yield the late eruptions of hawaiitic magmas [Frey *et al.*, 1990]. During the final, rejuvenated stage, however, no significant magma storage systems appear to exist at all and sporadically supplied strongly alkalic magmas appear to transit directly from upper mantle depths to the surface [e.g., Clague, 1987]. It is not always evident, however, to what extent this idealized Hawaiian relationship between magma supply rates and configuration of the magma plumbing system applies to other ocean island volcanoes, such as the Canary Islands [cf. Hoernle and Schmincke, 1993; Carracedo *et al.*, 1998].

[31] Volcanoes in their shield stage, such as Kilauea, Mauna Loa and, to a lesser extent, Piton de la Fournaise, may indeed be characterized by high magma supply rates and feature shallow magma reservoirs [Dvorak and Dzurisin, 1997; Peltier *et al.*, 2007]. Yet, other intraplate volcanoes apparently in their shield stage, such as those of the Atlantic islands of La Palma, El Hierro, Fogo, and Madeira, have low magma fluxes and, accordingly, tend to lack a shallow plumbing system [Amelung and Day, 2002; Schwarz *et al.*, 2004; Klügel *et al.*, 2005; Stroncik *et al.*, submitted manuscript, 2008]. The largely similar magma plumbing system geometry at the Atlantic localities suggests that it might be a characteristic feature of volcanoes in their shield-building stage situated on slow-moving plates and fed by relatively weak plumes. Therefore as suggested by several previous authors [e.g., Carracedo *et al.*, 1998; Klügel and Klein, 2006], the vigor of the mantle plume, the lithospheric thickness and the velocity of the moving oceanic plate probably play a major role in defining singularities at intraplate volcano chains.

[32] It appears, however, that a wider spectrum of mechanisms is required to explain discrepancies at individual volcanoes. Amelung and Day [2002] noted further departures from the general Hawaiian pattern at the Galapagos volcanoes, which, in spite of their relatively low magma supply rates, maintain shallow magma reservoirs. These authors proposed that the occurrence of “recent” giant mass-wasting events may explain the lack of shallow reservoirs at volcanoes with high magma fluxes. Conversely, the absence of such giant landslides in the recent geologic past of volcanoes with relatively low magma supply rates may allow the formation of a shallow plumbing system.

[33] As previously mentioned, Teno’s apparent lack of extensive shallow magma chambers at the time of emplacement of the El Palmar Formation is consistent with the situation of many Atlantic volcanoes in their shield-building stage. However, it also strongly resembles the postshield stage of Mauna Kea volcano [Frey *et al.*, 1990]. The oldest subaerial volcanics at Teno, the Masca Formation, are found stratigraphically below the two angular unconformities that represent the giant landslide scarps. This sequence includes a thick vitric tuff of trachytic composition (64.6 wt %  $\text{SiO}_2$ ) near its top, suggesting the temporary presence of an evolved shallow magma plumbing system earlier in the

volcano’s evolution (Longpré *et al.*, submitted manuscript, 2008).

[34] Miocene magma supply rates at Teno were on the order of  $\sim 1$  km<sup>3</sup>/ka [Leonhardt and Soffel, 2006], comparable to values for the Galapagos volcanoes [Naumann and Geist, 2000, and references therein], and the large volumes of the Carrizales and El Palmar formations are not consistent with a reduced supply rate after the emplacement of the Masca Formation. We therefore propose that the lack of a shallow plumbing system at the time of emplacement of the El Palmar Formation may be linked to the occurrence of two lateral collapses of the Teno volcano. The rapid unloading of several tens of km<sup>3</sup> of near-surface rocks may have provoked the opening of new magma pathways upon re-arrangement of the local volcano-tectonic stress field. Resulting pyroclastic eruptions appear to have accompanied collapse (Longpré *et al.*, submitted manuscript, 2008) and may be responsible for the drainage of shallow magma chambers.

#### 4.4. Controls on Magma Storage and Transport

[35] Magma transport is thought to be controlled by contrasts in the densities and/or thermomechanical properties of the host rocks [see Clague and Dixon, 2000; Klügel *et al.*, 2005, and references therein].

[36] The crust-mantle boundary marks an important density contrast in the lithosphere. On the margins of Tenerife, the Moho is located at depths between 13 and 15 km below sea level [Banda *et al.*, 1981; Watts *et al.*, 1997]. Seismically, however, the crust-mantle boundary may be a thick transition zone rather than a thin discontinuity under some parts of the Canary Islands, as demonstrated for Gran Canaria and, to a lesser extent, Tenerife [Ye *et al.*, 1999; Dañobeitia and Canales, 2000]. In any case and even though their buoyancy may significantly decrease in the lower crust [e.g., Takada, 1989], ascending magmas are not necessarily expected to stagnate at the Moho due to the apparent lack of a level of neutral buoyancy at this interface [e.g., Hansteen *et al.*, 1998]. However, once established for one reason or another, magma reservoirs at near-Moho depths may damp the ascent of subsequent magma batches [e.g., Clague, 1987].

[37] The long-term elastic thickness of the lithosphere ( $T_e$ ) may be related to a significant thermomechanical boundary [cf. Bodine *et al.*, 1981; Putirka, 1997]. At Loihi and Mauna Kea volcanoes, Hawaii, Putirka [1997] noticed that the shallowest magma storage depth estimates extracted from thermobarometric data coincide with estimates of  $T_e$ . This author proposed that a change in the mechanical behavior of the lithosphere below  $T_e$  inhibits fracture transport of magma. In the Canary Islands, estimates of  $T_e$  have been matter of substantial debate [see Collier and Watts, 2001]. Early estimates of the lithosphere’s effective elastic thickness ranged from 20 km [Watts, 1994] to 48 km [Filmer and McNutt, 1989]. However, Dañobeitia *et al.* [1994] subsequently proposed a best fit  $T_e$  of 35 km. Collier and Watts [2001] also argued that a  $T_e$  of 35 km is most likely, in agreement with values predicted by the cooling plate models [see, e.g., Watts and Zhong, 2000, and references therein]. This implies that the thermal effects associated with the Canary hot spot have not significantly weakened the lithosphere under the Canary Islands [see

also *Canales and Dañobeitia*, 1998]. Therefore for the purpose of this discussion, we place the postulated thermo-mechanical contrast at a depth of  $\sim 39$  km below sea level (depth =  $T_e$  + approximated water depth (4 km)). This depth estimate compares well with hypocenters [*Instituto Geográfico Nacional data*, 1975–2007], which cluster above a depth of ( $\sim 40$  km below sea level for 91% of calculated events and may indeed indicate a change in the thermomechanical behavior of the lithosphere at this level (Figure 4c).

[38] Taking into account the depth range yielded by our thermobarometric calculations (20–45 km), it seems that magma storage beneath the Teno volcano was largely confined from a few kilometers below the Moho to the base of the long-term elastic lithosphere in the upper mantle. This therefore differs from the Hawaiian case, where  $T_e$  appears to provide an upper as opposed to a lower bound to magma storage [cf. *Putirka*, 1997]. If a thermomechanical contrast controls the upper limit of magma stagnation, its association with  $T_e$  is thus not universal and may merely be accidental at Loihi and Mauna Kea. An attractive alternative explanation for the upper limit of magma storage at Teno may be found in the flexural model of *ten Brink and Brocher* [1987]. Flexural stresses deviating from lithostatic pressure (deviatoric stresses) are produced by the load of the volcanic edifice; the upper and lower parts of the lithosphere are in deviatoric compression and tension, respectively [*ten Brink and Brocher*, 1987]. As deviatoric compressive stresses overcome magma pressure in ascending dike tips, magma stagnation (and sill formation) may be promoted. This mechanism has been demonstrated to successfully account for the occurrence of plutonic complexes near the crust-mantle boundary under Hawaiian Islands; a situation that can probably be extrapolated to the Canary Archipelago [*ten Brink and Brocher*, 1987; *Dañobeitia and Canales*, 2000]. In turn, the deviatoric tensional stresses inferred to exist in the lower part of the elastic lithosphere may favor the formation of cracks, assuming equal magma and lithostatic pressure at this level [*Weertman*, 1971]. This may help channel magma into the lower elastic lithosphere. Combined together, these mechanisms may create an efficient magma trap in the lower long-term elastic lithosphere. We therefore propose that the upper limit of magma storage found at Teno and potentially at many other ocean island volcanoes with relatively low magma fluxes may be governed by compressive flexural stresses in the upper part of the elastic lithosphere. In addition, the occurrence of deviatoric tensional stresses in the lower part of the elastic lithosphere may explain the bottom limit given by our thermobarometric data. In this scenario, vertical intrusions (and potential subsequent eruptions) occur as magma pressure increases sufficiently due to degassing and/or crystallization to overcome the horizontal compressive stresses due to edifice load [*ten Brink and Brocher*, 1987].

[39] Available geophysical evidence for magmatic underplating in the Canary Archipelago is ambiguous [see *Watts et al.*, 1997; *Ye et al.*, 1999; *Dañobeitia and Canales*, 2000], as opposed to other intraplate ocean islands (e.g., Hawaii, Marquesas, La Réunion) [*Watts et al.*, 1985; *Caress et al.*, 1995; *Charvis et al.*, 1999]. However, our data corroborate evidence from other petrological studies [*Hansteen et al.*, 1998; *Klügel et al.*, 2005], suggesting that sub-Moho mafic

magmatic intrusions must contribute considerably to crustal thickening under Canarian volcanoes.

[40] The fact that hypocenters beneath the Canary Islands appear to extend significantly deeper than the long-term elastic thickness of the plate and beyond the probable 600°C isotherm (extent of mantle earthquakes [see *McKenzie et al.*, 2005, Figure 7]) may imply that CO<sub>2</sub>-rich fluids liberated by ascending magmas enable brittle failure through elevated pore fluid pressures [*Wilshire and Kirby*, 1989]. Such mechanism may provide independent evidence for magma storage and transport at upper mantle depths beneath the Canary Islands.

## 5. Summary

[41] Petrographic observations and major element chemistry of clinopyroxene phenocrysts show that thin darker rims, commonly hosting acicular apatite microcrystals and sometimes displaying dendritic protrusions, are coupled with steep normal Fe-Mg zoning and drastic TiO<sub>2</sub> enrichment. Combined with similar zonations in olivine, these observations suggest that the outer rims formed due to decompression-induced crystallization upon rapid magma ascent and accompanying degassing and undercooling. This process took place under disequilibrium conditions as shown by our equilibrium tests, implying that clinopyroxene rim compositions may not always be suitable for thermobarometric investigations. Magma storage under the Teno shield-volcano at the time of the emplacement of the El Palmar Formation took place well into the uppermost mantle, at depths between 20 and 45 km below present sea level. Giant mass-wasting events earlier in the volcano's evolution may have re-arranged local stress fields, initiating the formation of new magma pathways and leading to the permanent extinction of shallow crustal magma reservoirs. Our data reveal the presence of a magma trap at depth that may be due to either thermomechanical contrasts or the influence of deviatoric bending stresses in the elastic lithosphere. In the latter scenario, horizontal compressive stresses may promote sill formation, perhaps fortuitously, just below the crust-mantle boundary, thus providing a mechanism for progressive magmatic underplating in the Canary Archipelago. The combination of a careful sampling strategy, petrography, mineral chemistry and clinopyroxene thermobarometry provides a promising approach to the investigation of magma plumbing systems at basaltic volcanoes.

[42] **Acknowledgments.** We thank J. Chadwick (Vrije U.), S. Jones (TCD), J. Maclennan (U. Cambridge), T. Walter, A. Manconi (GFZ Potsdam) and especially A. Klügel (U. Bremen) for stimulating discussions. We also acknowledge G. Brey (U. Frankfurt) for providing the shock-melting experiment logistics and M. Thöner (IFM-GEOMAR) for EMP analytical support. This paper benefited from constructive and thoughtful reviews by K. Putirka and T. Sisson and editorial handling by J. Foden. Financial support to M.-A.L. was provided through a Natural Science and Engineering Research Council of Canada Scholarship and a Trinity Postgraduate Studentship and to V.R.T. by Science Foundation Ireland and Trinity College Dublin.

## References

- Ablay, G., M. R. Carroll, M. R. Palmar, J. Martí, and S. J. Sparks (1998), Basanite-phonolite lineages of the Teide-Pico Viejo volcanic complex, Tenerife, Canary Islands, *J. Petrol.*, 39, 905–936.

- Abratis, M., H.-U. Schmincke, and T. H. Hansteen (2002), Composition and evolution of submarine volcanic rocks from the central and western Canary Islands, *Int. J. Earth Sci.*, *91*, 562–582.
- Amelung, F., and S. Day (2002), InSAR observations of the 1995 Fogo, Cape Verde, eruption: Implications for the effects of collapse events upon island volcanoes, *Geophys. Res. Lett.*, *29*(12), 1606, doi:10.1029/2001GL013760.
- Andronico, D., et al. (2005), A multi-disciplinary study of the 2002–03 Etna eruption: Insights into a complex plumbing system, *Bull. Volcanol.*, *67*, 314–330.
- Banda, E., J. J. Dañoibeitia, E. Suriñach, and J. Ansoerge (1981), Features of crustal structure under the Canary Islands, *Earth Planet. Sci. Lett.*, *55*, 11–24.
- Beattie, P. (1993), Olivine-melt and orthopyroxene-melt equilibria, *Contrib. Mineral. Petrol.*, *115*, 103–111.
- Blundy, J., and K. Cashman (2005), Rapid decompression-driven crystallization recorded by melt inclusions from Mount St. Helens volcano, *Geology*, *33*, 793–796.
- Bodine, J. H., M. S. Steckler, and A. B. Watts (1981), Observations of flexure and the rheology of the oceanic lithosphere, *J. Geophys. Res.*, *86*, 3695–3707.
- Canales, J. P., and J. J. Dañoibeitia (1998), The Canary Islands swell: A coherence analysis of bathymetry and gravity, *Geophys. J. Int.*, *132*, 479–488.
- Caress, D. W., M. K. McNutt, R. S. Detrick, and J. C. Mutter (1995), Seismic imaging of hotspot-related crustal underplating beneath the Marquesas Islands, *Nature*, *373*, 600–602.
- Carracedo, J. C., S. Day, H. Guillou, E. Rodríguez Badiola, J. A. Canas, and F. J. Pérez Torrado (1998), Hotspot volcanism close to a passive continental margin: The Canary Islands, *Geol. Mag.*, *135*, 591–604.
- Carracedo, J. C., E. Rodríguez Badiola, H. Guillou, M. Paterne, S. Scaillet, F. J. Pérez Torrado, R. Paris, U. Fra-Paleo, and A. Hansen (2007), Eruptive and structural history of Teide Volcano and rift zones of Tenerife, Canary Islands, *Geol. Soc. Am. Bull.*, *119*, 1027–1051.
- Charvis, P., A. Laesanpura, J. Gallart, A. Hirn, J. C. Lépine, B. de Voogd, T. A. Minshall, Y. Hello, and B. Pontoise (1999), Spatial distribution of hotspot material added to the lithosphere under La Réunion, from wide-angle seismic data, *J. Geophys. Res.*, *104*, 2875–2893.
- Clague, D. A. (1987), Hawaiian xenolith populations, magma supply rates, and development of magma chambers, *Bull. Volcanol.*, *49*, 577–587.
- Clague, D. A., and J. E. Dixon (2000), Extrinsic controls on the evolution of Hawaiian ocean island volcanoes, *Geochem. Geophys. Geosyst.*, *1*(4), 1010, doi:10.1029/1999GC000023.
- Collier, J. S., and A. B. Watts (2001), Lithospheric response to volcanic loading by the Canary Islands: Constraints from seismic reflection data in their flexural moat, *Geophys. J. Int.*, *147*, 660–676.
- Dañoibeitia, J. J., and J. P. Canales (2000), Magmatic underplating in the Canary Archipelago, *J. Volcanol. Geotherm. Res.*, *103*, 27–41.
- Dañoibeitia, J. J., J. P. Canales, and G. A. Dehghani (1994), An estimation of the elastic thickness of the lithosphere in the Canary Archipelago using admittance function, *Geophys. Res. Lett.*, *21*, 2649–2652.
- Dixon, J. E. (1997), Degassing of alkalic basalts, *Am. Mineral.*, *82*, 368–378.
- Droop, G. T. R. (1987), A general equation for estimating Fe<sup>3+</sup> concentrations in ferromagnesian silicates and oxides from microprobe analyses, using stoichiometric criteria, *Mineral. Mag.*, *51*, 431–435.
- Duke, J. M. (1976), Distribution of the period four transition elements among olivine, calcic clinopyroxene and mafic silicate liquid: Experimental results, *J. Petrol.*, *17*, 499–521.
- Dvorak, J. J., and D. Dzurisin (1997), Volcano geodesy: The search for magma reservoirs and the formation of eruptive vents, *Rev. Geophys.*, *35*, 343–384.
- Filmer, P. E., and M. K. McNutt (1989), Geoid anomalies over the Canary Islands Group, *Mar. Geophys. Res.*, *11*, 77–87.
- Freer, R. (1981), Diffusion in silicate minerals: A data digest and guide to the literature, *Contrib. Mineral. Petrol.*, *76*, 440–454.
- Frey, F. A., W. S. Wise, M. O. Garcia, H. West, S.-T. Kwon, and A. Kennedy (1990), Evolution of Mauna Kea Volcano, Hawaii: Petrologic and geochemical constraints on postshield volcanism, *J. Geophys. Res.*, *95*, 1271–1300.
- Ghiorso, M. S., and R. O. Sack (1995), Chemical transfer in magmatic processes. part IV: A revised and internally consistent thermodynamic model for the interpolation and extrapolation of liquid–solid equilibria in magmatic systems at elevated temperatures and pressures, *Contrib. Mineral. Petrol.*, *119*, 197–212.
- Greenwood, J. C. (2001), The secular geochemical variation of the Trinidad mantle plume, Ph.D. thesis, 292 pp., Univ. of Cambridge, Cambridge, U.K.
- Gudmundsson, A., L. B. Marinoni, and J. Martí (1999), Injection and arrest of dikes: Implications for volcanic hazards, *J. Volcanol. Geotherm. Res.*, *88*, 1–13.
- Guillou, H., J. C. Carracedo, R. Paris, and F. J. Pérez Torrado (2004), Implications for the early shield-stage evolution of Tenerife from K/Ar ages and magnetic stratigraphy, *Earth Planet. Sci. Lett.*, *222*, 599–614.
- Gurenko, A. A., and H.-U. Schmincke (2000), S concentrations and its speciation in Miocene basaltic magmas north and south of Gran Canaria (Canary Islands): Constraints from glass inclusions in olivine and clinopyroxene, *Geochim. Cosmochim. Acta*, *64*, 2321–2337.
- Gurenko, A. A., T. H. Hansteen, and H.-U. Schmincke (1996), Evolution of parental magmas of Miocene shield basalts of Gran Canaria (Canary Islands): Constraints from crystal, melt and fluid inclusions in minerals, *Contrib. Mineral. Petrol.*, *124*, 422–435.
- Hansteen, T. H., A. Klügel, and H.-U. Schmincke (1998), Multi-stage magma ascent beneath the Canary Islands: Evidence from fluid inclusions, *Contrib. Mineral. Petrol.*, *132*, 48–64.
- Hoernle, K. A. J., and H.-U. Schmincke (1993), The role of partial melting in the 15-ma geochemical evolution of Gran Canaria: A blob model for the Canary hotspot, *J. Petrol.*, *34*, 599–626.
- Humphreys, M. C. S., J. Blundy, and R. S. J. Sparks (2006), Magma evolution and open-system processes at Shiveluch volcano: Insights from phenocryst zoning, *J. Petrol.*, *47*, 2303–2334.
- Instituto Geográfico Nacional, Ministerio de Fomento, Servicio de Información Sísmica (1975–2007), *Catálogo y Boletines Sísmicos*, Retrieved on 29 July 2007 from: <http://www.ign.es/ign/es/IGN/SisCatalogo.jsp>.
- Klügel, A., and F. Klein (2006), Complex magma storage and ascent at embryonic submarine volcanoes from the Madeira Archipelago, *Geology*, *34*, 337–340.
- Klügel, A., K. A. Hoernle, H.-U. Schmincke, and J. D. L. White (2000), The chemically zoned 1949 eruption on La Palma (Canary Islands): Petrologic evolution and magma supply dynamics of a rift zone eruption, *J. Geophys. Res.*, *105*, 5997–6016.
- Klügel, A., T. H. Hansteen, and K. Galipp (2005), Magma storage and underplating beneath Cumbre Vieja volcano, La Palma (Canary Islands), *Earth Planet. Sci. Lett.*, *236*, 211–226.
- Kress, V. C., and I. S. E. Carmichael (1988), Stoichiometry of the iron oxidation reaction in silicate melts, *Am. Mineral.*, *73*, 1267–1274.
- Leonhardt, R., and H. C. Soffel (2006), The growth, collapse and quiescence of Tenno volcano, Tenerife: New constraints from paleomagnetic data, *Int. J. Earth Sci.*, *95*, 1053–1064.
- Lindsley, D. H. (1983), Pyroxene thermometry, *Am. Mineral.*, *68*, 477–493.
- Lipman, P. W., N. G. Banks, and J. M. Rhodes (1985), Degassing-induced crystallization of basaltic magma and effects on lava rheology, *Nature*, *317*, 604–607.
- Lofgren, G. (1974), An experimental study of plagioclase crystal morphology: Isothermal crystallization, *Am. J. Sci.*, *274*, 243–273.
- MacLennan, J., D. McKenzie, K. Gronvold, and L. Slater (2001), Crustal accretion under northern Iceland, *Earth Planet. Sci. Lett.*, *191*, 295–310.
- Marsh, B. D. (1996), Solidification fronts and magmatic evolution, *Mineral. Mag.*, *60*, 5–40.
- Martí, J., J. Mitjavila, and V. Araña (1994), Stratigraphy, structure and geochronology of the Las Cañadas caldera (Tenerife, Canary Islands), *Geol. Mag.*, *131*, 715–727.
- McGuire, A. V., M. D. Dyar, and K. A. Ward (1989), Neglected Fe<sup>3+</sup>/Fe<sup>2+</sup> ratios—A study of Fe<sup>3+</sup> content of megacrysts from alkali basalts, *Geology*, *17*, 687–690.
- McKenzie, D., and M. J. Bickle (1988), The volume and composition of melt generated by extension of the lithosphere, *J. Petrol.*, *29*, 625–679.
- McKenzie, D., J. Jackson, and K. Priestley (2005), Thermal structure of oceanic and continental lithosphere, *Earth Planet. Sci. Lett.*, *233*, 337–349.
- Mordick, B. E., and A. F. Glazner (2006), Clinopyroxene thermobarometry of basalts from the Coso and Big Pine volcanic fields, California, *Contrib. Mineral. Petrol.*, *152*, 111–124.
- Naumann, T., and D. Geist (2000), Physical volcanology and structural development of Cerro Azul Volcano, Isabela Island, Galápagos: Implications for the development of Galápagos-type shield volcanoes, *Bull. Volcanol.*, *61*, 497–514.
- Neumann, E.-R. (1991), Ultramafic and mafic xenoliths from Hierro, Canary Islands: Evidence for melt infiltration in the upper mantle, *Contrib. Mineral. Petrol.*, *106*, 236–252.
- Neumann, E.-R., E. Wulff-Pedersen, S. L. Simonsen, N. J. Pearson, J. Martí, and J. Mitjavila (1999), Evidence for fractional crystallization of periodically refilled magma chambers in Tenerife, Canary Islands, *J. Petrol.*, *40*, 1089–1123.
- O'Hara, M. J. (1977), Geochemical evolution during fractional crystallization of a periodically refilled magma chamber, *Nature*, *266*, 503–507.

- Olafsson, M., and D. H. Eggler (1983), Phase relations of amphibole, amphibole-carbonate, and phlogopite-carbonate peridotite: Petrologic constraints on the asthenosphere, *Earth Planet. Sci. Lett.*, *64*, 305–315.
- Pallister, J. S., R. P. Hoblitt, D. R. Crandell, and D. R. Mullineaux (1992), Mount St. Helens a decade after the 1980 eruptions: Magmatic models, chemical cycles, and a revised hazards assessment, *Bull. Volcanol.*, *54*, 126–146.
- Peltier, A., T. Staudacher, and P. Bachèlery (2007), Constraints on magma transfers and structures involved in the 2003 activity at Piton de La Fournaise from displacement data, *J. Geophys. Res.*, *112*, B03207, doi:10.1029/2006JB004379.
- Perugini, D., T. Busa, G. Poli, and S. Nazzareni (2003), The role of chaotic dynamics and flow fields in the development of disequilibrium textures in volcanic rocks, *J. Petrol.*, *44*, 733–756.
- Putirka, K. (1997), Magma transport at Hawaii: Inferences based on igneous thermobarometry, *Geology*, *25*, 69–72.
- Putirka, K. (1999), Clinopyroxene + liquid equilibria to 100 kbar and 2450 K, *Contrib. Mineral. Petrol.*, *135*, 151–163.
- Putirka, K., M. Johnson, R. Kinzler, J. Longhi, and D. Walker (1996), Thermobarometry of mafic igneous rocks based on clinopyroxene-liquid equilibria, 030 kbar, *Contrib. Mineral. Petrol.*, *123*, 92–108.
- Putirka, K., H. Mikaelian, F. Ryerson, and H. Shaw (2003), New clinopyroxene-liquid thermobarometers for mafic, evolved, and volatile-bearing lava compositions, with applications to lavas from Tibet and the Snake River Plain, Idaho, *Am. Mineral.*, *88*, 1542–1554.
- Ranero, C. R., M. Torne, and E. Banda (1995), Gravity and multichannel seismic reflection constraints on the lithospheric structure of the Canary Swell, *Mar. Geophys. Res.*, *17*, 519–534.
- Roeder, P. L., and R. F. Emslie (1970), Olivine-liquid equilibrium, *Contrib. Mineral. Petrol.*, *29*, 275–289.
- Rutherford, M. J., H. Sigurdsson, S. Carey, and A. Davis (1985), The May 18, 1980, eruption of Mount St. Helens. I-Melt composition and experimental phase equilibria, *J. Geophys. Res.*, *90*, 2929–2947.
- Sachs, P. M., and T. H. Hansteen (2000), Pleistocene underplating and metasomatism of the lower continental crust: A xenolith study, *J. Petrol.*, *41*, 331–356.
- Schwarz, S., A. Klügel, and C. Wohlgemuth-Ueberwasser (2004), Melt extraction pathways and stagnation depths beneath the Madeira and Desertas rift zones (NE Atlantic) inferred from barometric studies, *Contrib. Mineral. Petrol.*, *147*, 228–240.
- Soesoo, A. (1997), A multivariate statistical analysis of clinopyroxene composition: Empirical coordinates for the crystallization PT-estimations, *GFF (Geol. Föeren. Föerh.)*, *119*, 55–60.
- Sparks, R. S. J., and H. Pinkerton (1978), Effect of degassing on rheology of basaltic lava, *Nature*, *276*, 385–386.
- Takada, A. (1989), Magma transport and reservoir formation by a system of propagating cracks, *Bull. Volcanol.*, *52*, 118–126.
- ten Brink, U. S., and T. M. Brocher (1987), Multichannel seismic evidence for a subcrustal intrusive complex under Oahu and a model for Hawaiian volcanism, *J. Geophys. Res.*, *92*, 13,687–13,707.
- Thirlwall, M. F., B. S. Singer, and G. F. Marriner (2000), <sup>39</sup>Ar-<sup>40</sup>Ar ages and geochemistry of the basaltic shield stage of Tenerife, Canary Islands, Spain, *J. Volcanol. Geotherm. Res.*, *103*, 247–297.
- Thompson, R. N. (1974), Some high-pressure pyroxenes, *Mineral. Mag.*, *39*, 768–787.
- Tilling, R. I., and J. J. Dvorak (1993), Anatomy of a basaltic volcano, *Nature*, *363*, 125–133.
- Troll, V. R., and H.-U. Schmincke (2002), Magma mixing and crustal recycling recorded in ternary feldspar from compositionally zoned per-alkaline ignimbrite “A”, Gran Canaria, Canary Islands, *J. Petrol.*, *43*, 243–270.
- Walter, T., and H.-U. Schmincke (2002), Rifting, recurrent landsliding and Miocene structural reorganization on NW-Tenerife (Canary Islands), *Int. J. Earth Sci.*, *91*, 615–628.
- Wass, S. Y. (1979), Multiple origins of clinopyroxenes in alkali basaltic rocks, *Lithos*, *12*, 115–132.
- Watts, A. B. (1994), Crustal structure, gravity anomalies and flexure of the in the vicinity of the Canary Islands, *Geophys. J. Int.*, *119*, 648–666.
- Watts, A. B., and S. Zhong (2000), Observations of flexure and the rheology of oceanic lithosphere, *Geophys. J. Int.*, *142*, 855–875.
- Watts, A. B., U. S. ten Brink, P. Buhl, and T. M. Brocher (1985), A multichannel seismic study of lithospheric flexure across the Hawaiian-Emperor seamount chain, *Nature*, *315*, 105–111.
- Watts, A. B., C. Peirce, J. Collier, R. Dalwood, J. P. Canales, and T. J. Henstock (1997), A seismic study of lithospheric flexure in the vicinity of Tenerife, Canary Islands, *Earth Planet. Sci. Lett.*, *146*, 431–447.
- Weertman, J. (1971), Theory of water-filled crevasses in glaciers applied to vertical magma transport beneath oceanic ridges, *J. Geophys. Res.*, *76*, 1171–1183.
- Wilshire, H. G., and S. H. Kirby (1989), Dikes, joints, and faults in the upper mantle, *Tectonophysics*, *161*, 23–31.
- Wyllie, P. J., K. G. Cox, and G. M. Biggar (1962), The habit of apatite in synthetic systems and igneous rocks, *J. Petrol.*, *3*, 238–243.
- Ye, S., J. P. Canales, R. Rihm, J. J. Dañobeitia, and J. Gallart (1999), A crustal transect through the northern and northeastern part of the volcanic edifice of Gran Canaria, Canary Islands, *J. Geodyn.*, *28*, 3–26.

T. H. Hansteen, IFM-GEOMAR, Leibniz-Institut für Meereswissenschaften, Wischhofstr. 1-3, D-24148 Kiel, Germany.

M.-A. Longpré, Department of Geology, Trinity College Dublin, College Green, Dublin 2, Ireland. (longprem@tcd.ie)

V. R. Troll, Department of Earth Sciences, Uppsala Universitet, Villavägen 16, SE-752 36 Uppsala, Sweden.